

Supporting Information

DLP 3D printing of electronically conductive hybrid hydrogels via polymerization-induced phase separation and subsequent in-situ assembly of polypyrrole

Chuhan Song^{1,2}, Qian Zhao², Tao Xie², Jingjun Wu^{1,2}*

1Ningbo Innovation Center, Zhejiang University, Ningbo 315807, China

2State Key Laboratory of Chemical Engineering, College of Chemical and Biological Engineering, Zhejiang University, Hangzhou 310027, China

*Correspondence: jingjunwu@zju.edu.cn

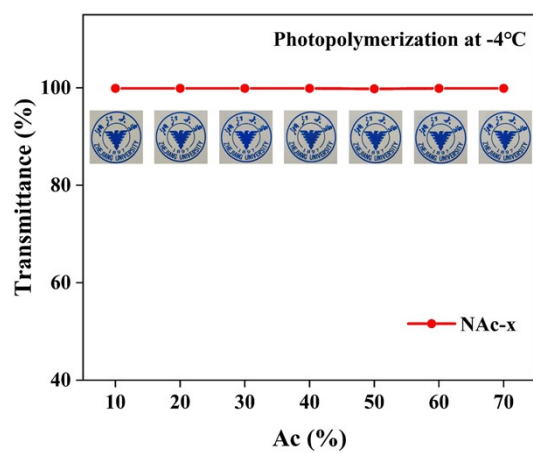
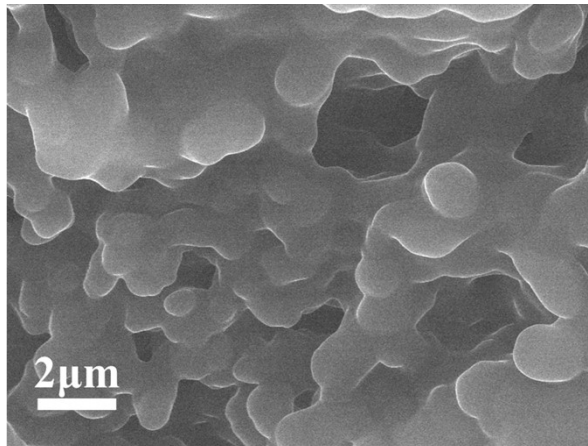


Figure S1. Transmittance of hydrogels with different Ac ratios for photoinitiated polymerization at -4 °C.



NAc-50

Figure S2. FESEM image of NAc-50. The electron microscope image is based on the cross section of the hydrogel sample.

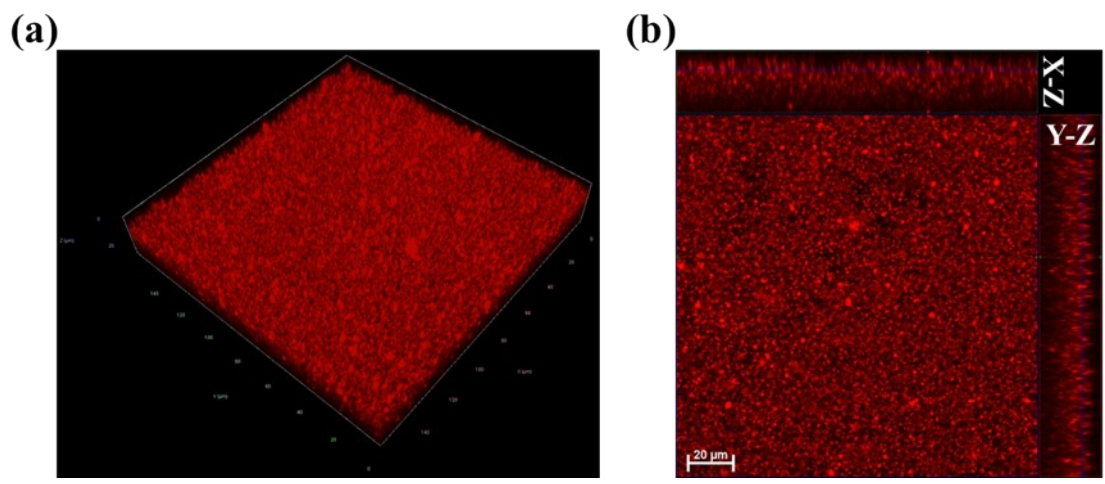


Figure S3. (a) Laser confocal microscope 3D contour image of NAc-50 porous hydrogel. (b) Top view, X-Z profile and Y-Z profile of NAc-50 porous hydrogel by laser confocal microscopy.

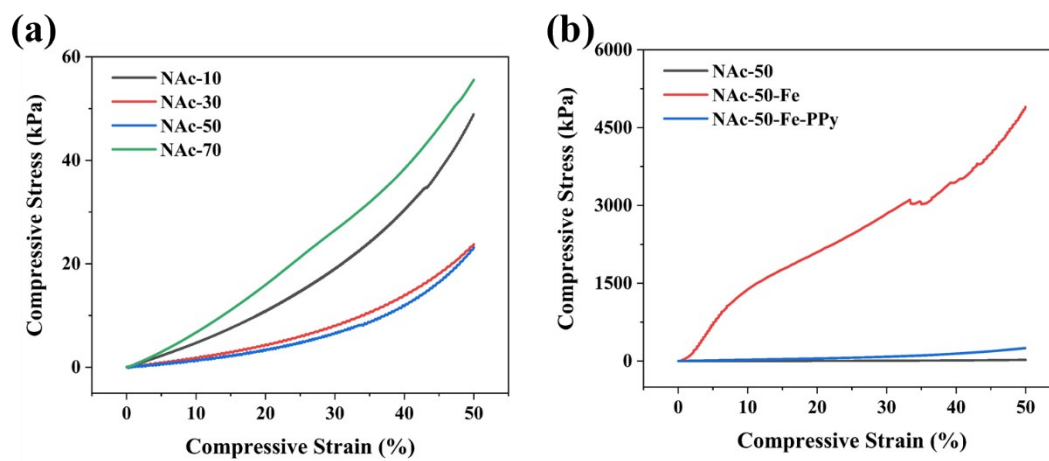


Figure S4. (a) Mechanical test of hydrogels of NIPAm and Ac with different compositions. (b) Mechanical test of hydrogels of NAc-50, NAc-50-Fe and NAc-50-Fe-PPy sample.

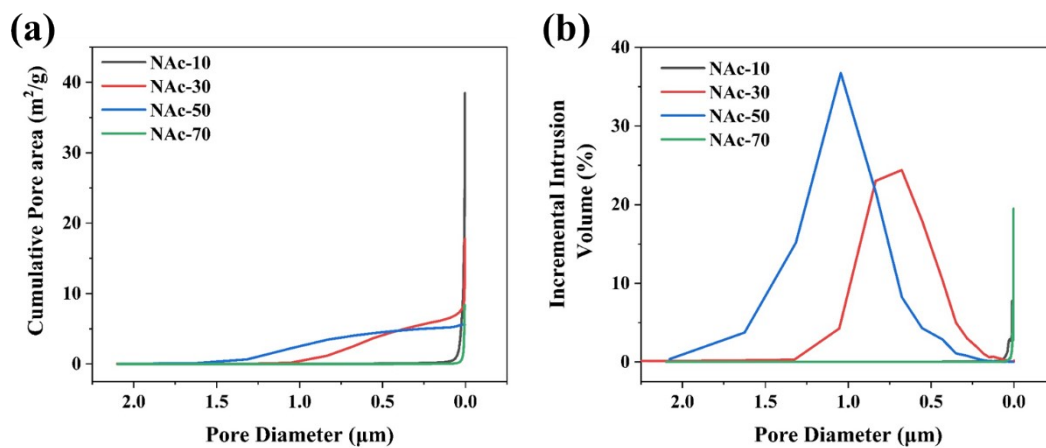


Figure S5. (a) Cumulative pore area of dried hydrogels with different compositions. (b) Pore size distribution of dried hydrogels with different compositions.

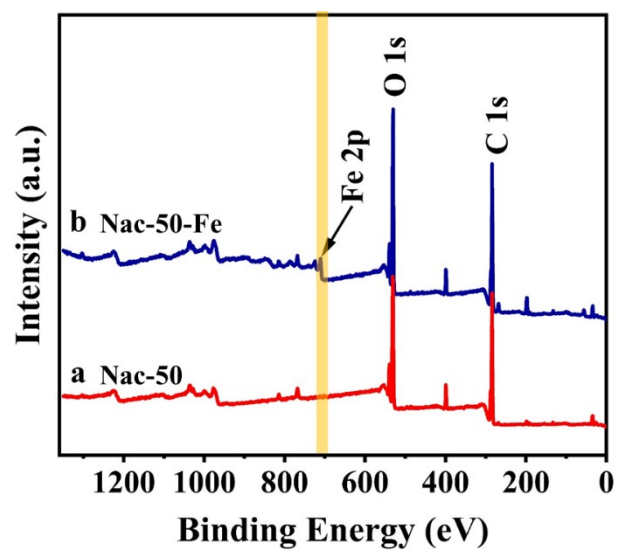


Figure S6. XPS spectra of NAc-50 and NAc-50-Fe porous hydrogels.

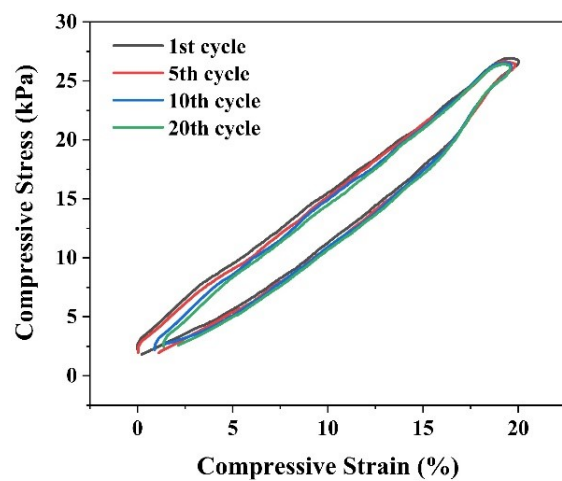


Figure S7. Cyclic mechanical test of NAc-50-Fe-PPy hydrogel.

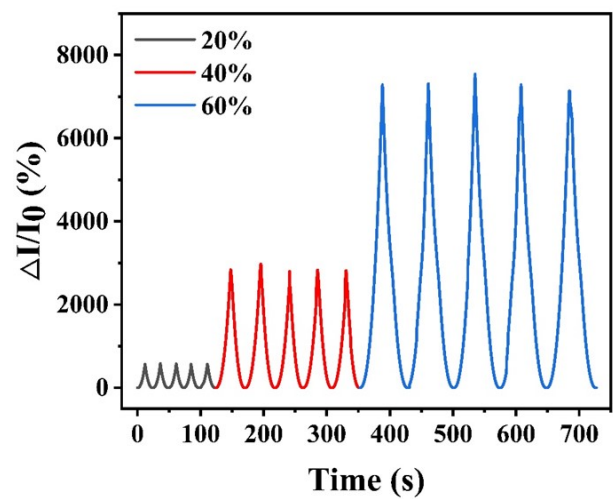


Figure S8. Piezoresistive properties of NAc-50-Fe-PPy piezoresistive sensor with low density lattice at different compression amplitudes.

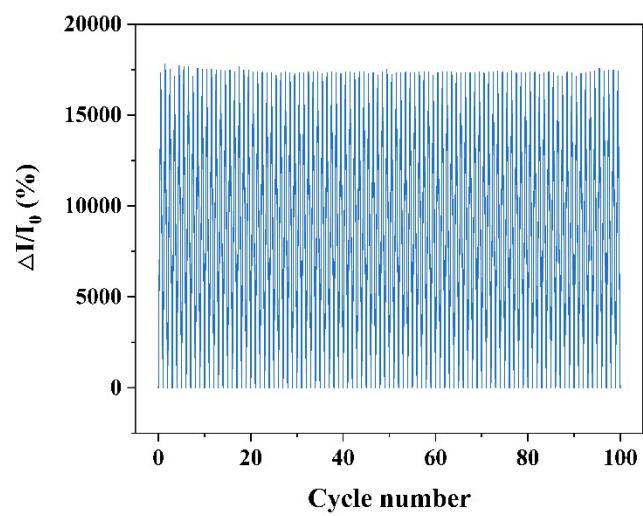


Figure S9. Long-term stability of NAc-50-Fe-PPy piezoresistive sensor at 20% strain.